Molecular Therapy
Nucleic Acids
Original Article

Secreted PGK1 and IGFBP2 contribute to the bystander effect of miR-10b gene editing in glioma

Yanhong Zhang,[1,3] Rosalia Rabinovsky,[1,3] Zhiyun Wei,[1] Rachid El Fatimy,[1] Evgeny Deforzh,[1] Bai Luan,[2] Leonid Peshkin,[2] Erik J. Uhlmann,[1] and Anna M. Krichevsky[1]

[1]Department of Neurology, Brigham and Women's Hospital and Harvard Medical School, Harvard Initiative for RNA Medicine, Boston, MA 02115, USA; [2]Department of Systems Biology, Harvard Medical School, Boston, MA 02115, USA

MicroRNA-10b (miR-10b) is an essential glioma driver and one of the top candidates for targeted therapies for glioblastoma and other cancers. This unique miRNA controls glioma cell cycle and viability via an array of established conventional and unconventional mechanisms. Previously reported CRISPR-Cas9-mediated miR-10b gene editing of glioma cells *in vitro* and established orthotopic glioblastoma in mouse models demonstrated the efficacy of this approach and its promise for therapy development. However, therapeutic gene editing in patients' brain tumors may be hampered, among other factors, by the imperfect delivery and distribution of targeting vectors. Here, we demonstrate that miR-10b gene editing in glioma cells triggers a potent bystander effect that leads to the selective cell death of the unedited glioma cells without affecting the normal neuroglial cells. The effect is mediated by the secreted miR-10b targets phosphoglycerate kinase 1 (PGK1) and insulin-like growth factor binding protein 2 (IGFBP2) that block cell-cycle progression and induce glioma cell death. These findings further support the feasibility of therapeutic miR-10b editing without the need to target every cell of the tumor.

INTRODUCTION

Glioblastoma (GBM), classified by WHO as a grade 4 glioma, is a highly malignant and the most common primary brain tumor in adults, accounting for almost 50% of all primary central nervous system (CNS) malignancies.[1] Treatment options are very limited and inefficient, and the 5-year survival rate is still only 5%–7%.[1] While there are multiple reasons for failures in the development of therapies for GBM, the heterogeneity of the disease and the lack of common oncogenic drivers is considered one of the major impeding factors.[2] Personalized molecular therapies have been proposed for GBM subtypes based on specific mutations and biomarkers, such as IDH and EGFR.[3,4] However, personalized strategies are challenging, considering the highly aggressive nature and fast progression of the disease, and may still not prove efficacious for the majority of patients with low mutation burden.[1]

An oncogenic microRNA-10b (miR-10b) was identified as a common therapeutic target for GBM and other malignant gliomas.[5–11] It belongs to a class of small non-coding RNA regulators, microRNAs (miRNAs), that control protein expression by direct binding, destabilization, and translational repression of mRNA targets.[12] Deregulated miRNAs play essential roles in tumorigenesis and may function as oncogenes and tumor suppressors.[13,14]

miR-10b is an established regulator of tumor cell growth and survival in glioma[5,7,9,10,15] and also exhibits a distinct tumorigenic and pro-metastatic activity in other cancers.[15–17] We and others have shown that miR-10b is silent in normal neuroglial cells of the brain and strongly induced in GBM.[5,6] Inhibition of miR-10b using two approaches, antisense oligonucleotides and CRISPR-based miR-10b gene editing, in heterogeneous glioma cells and GBM-initiating stem-like cells (GSCs) *in vitro* and orthotopic tumors *in vivo* suggested the efficacy and safety of therapeutic miR-10b targeting.[5,7,10] miR-10b is expressed in almost all human GBMs, and all tested highly diverse glioma xenograft and allograft models were sensitive to miR-10b inhibition. In contrast, normal neural cells were not affected by miR-10b inhibitors. Importantly, although the efficacy of the lentivirus-mediated CRISPR-Cas9-based miR-10b gene editing *in vitro* and *in vivo* was limited, its impact on the growth of glioma cultures and, most notably, on brain tumors was remarkable. In the first animal trial of gene editing for GBM *in vivo*, mice with established orthotopic GBMs that received miR-10b editing therapy exhibited tumor shrinkage and significant survival improvement.[10] These results, while paving the way for the therapeutic gene editing for currently incurable brain tumors, also suggested that bystander, non-cell-autonomous functions of miR-10b gene editing may contribute to the observed effects.

Here, we examined the hypothesis that miR-10b gene editing in glioma cells initiates a cascade reaction, inducing a potent killing of the neighboring tumor cells. To test the non-cell-autonomous

Received 8 August 2022; accepted 31 December 2022;
https://doi.org/10.1016/j.omtn.2022.12.018.

[3]These authors contributed equally

Correspondence: Anna M. Krichevsky, Ann Romney Center for Neurologic Diseases, Hale Building for Transformative Medicine, 60 Fenwood Rd, Room 9002T, Boston, MA 02115, USA.
E-mail: akrichevsky@bwh.harvard.edu

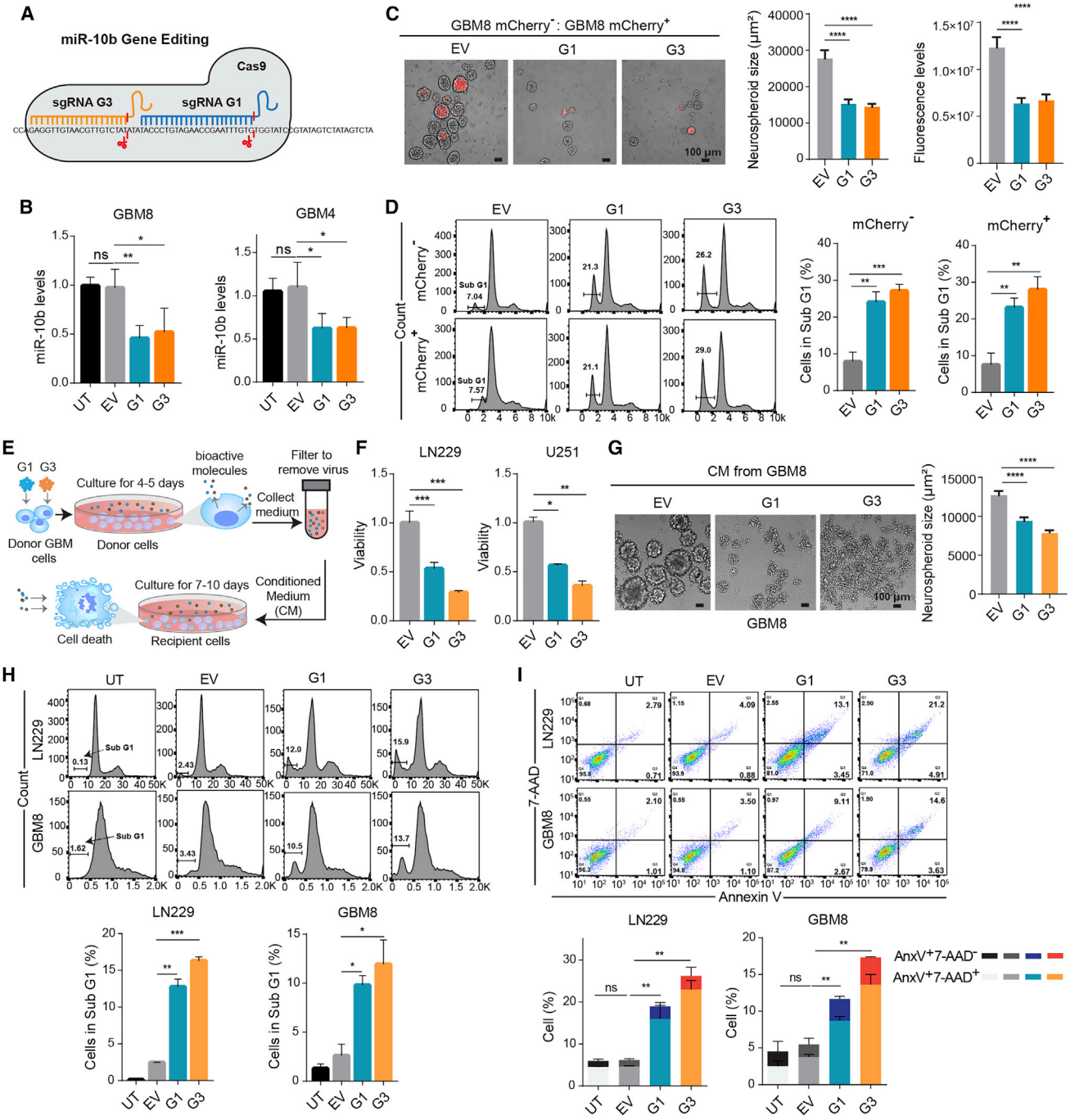

Figure 1. Bystander effect of miR-10b gene editing

(A) Schematic illustration of G1 and G3 sgRNAs for CRISPR-Cas9 miR-10b editing. The sgRNAs have been selected based on El Fatimy et al.[10] (B) miR-10b levels in GSC cultures transduced with low titers of either EV (Cas9 only) or miR-10b-editing G1 or G3 lentivirus, or untreated (UT), were analyzed by qRT-PCR (mean ± SD, n = 4 samples/group, two-tailed unpaired t test). The data were normalized to the levels of two unrelated, uniformly expressed miRNAs, miR-125a and miR-99a (geometrical mean). The experiment was repeated four times. (C and D) miR-10b-edited mCherry⁻ GBM8 cells, transduced with either G1 or G3 lentivirus, reduce the growth of naive mCherry⁺ GSCs in mixed cultures. Two cell populations, mCherry⁻ (partly edited) and mCherry⁺ (unedited) GSCs were mixed 1:1 and co-cultured for 7 days, and the resulting spheroids were analyzed. Representative images (C), cell-cycle analysis of sorted mCherry⁻ and mCherry⁺ cells (D), and data quantification are demonstrated (mean ± SEM, n = 5 samples/group, one-way ANOVA). (E) Illustration of the experimental design testing the effects of CM derived from miR-10b-edited or control glioma cells on recipient cultures. (F) Viability of naive glioma cell lines is inhibited by CM of miR-10b-edited cells. Naive LN229 and U251 cells were cultured for 7 days in CM collected from the corresponding

(legend continued on next page)

mechanism by which miR-10b editing leads to massive glioma cell death, we evaluated the conditioned media (CM) and secretome of the miR-10b-edited cells using an unbiased quantitative mass spectrometry. We demonstrate that miR-10b editing enhances the secretion of glioma death-promoting proteins. Among them, we identified phosphoglycerate kinase 1 (PGK1) and insulin-like growth factor binding protein 2 (IGFBP2) as the major contributing factors. These findings further support the development of the therapeutic miR-10b gene editing strategy for malignant gliomas.

RESULTS

Bystander effect of miR-10b gene editing

As previously reported, the moderate levels of CRISPR-Cas9-mediated miR-10b gene editing were sufficient to strongly reduce the viability of glioma cells and GSC spheroids and the growth of orthotopic GBM in mouse models.[10] Treatment of GBM cells with low-titer lentivirus (4×10^{-5} U/mL) resulted in about 40% of cell infections (Figure S1A). miR-10b gene editing with previously validated G1 single guide RNA (sgRNA; targeting mature miR-10b) or G3 sgRNA (targeting pri-miR-10b) resulted in deleterious mutations and 40%–50% reduction in miR-10b levels (Figures 1A, 1B, S1B, and S1C) and significantly inhibited the growth of glioma cells and GSCs (Figures S2A and S2B). In contrast, normal neuroglial cells such as human astrocytes and primary rat neurons, not expressing miR-10b, were unaffected by the miR-10b gene editing (Figure S2C; El Fatimy et al.[10]).

We hypothesized that the effects of miR-10b editing on glioma growth were not entirely cell autonomous and might be in part mediated by a bystander mechanism. To test this hypothesis, we edited miR-10b in GBM8 and GBM4 GSCs with the low-titer viruses, removed the viruses 24 h post-infection, and then mixed the dissociated cells with naive untreated mCherry$^+$ GSCs at a 1:1 ratio. Control cells infected with the lentivirus encoding Cas9 but not sgRNA (empty vector, EV) have been used in parallel. Both mCherry$^-$ (edited) and mCherry$^+$ (naive unedited) demonstrated the reduced capacity to form spheroids in the mixed cultures (Figures 1C and S3A). Furthermore, both cell populations were characterized by increased cell death, as demonstrated by cell sorting and analysis of the sub-G1 population (Figure 1D). This analysis suggested that miR-10b editing triggers the secretion of cell death-promoting factor(s).

To test this hypothesis, we collected CM from miR-10b-edited glioma cells targeted with either Cas9-sgRNA G1 (G1-CM) or Cas9-sgRNA G3 (G3-CM) and control cells infected with the lentivirus encoding Cas9 only (EV-CM). The CM samples were centrifuged to remove cell debris and filtered through the 0.1-μm filters to remove any traces of the lentivirus. The cleared CMs were then added to naive GSCs (GBM4 and GBM8) or glioma cell lines (LN229 and U251), as illustrated in Figure 1E's diagram. Culturing naive glioma cell lines with G1-CM or G3-CM resulted in 40%–60% reduced viability compared with EV-CM (Figures 1F and S3B). Similarly, CM from miR-10b-edited GSCs added to naive GBM8 cells reduced the growth of GSC spheroids (Figure 1G). The results were consistent for different combinations of the donor and recipient glioma cultures (Figure S3B). In contrast, CM of the edited glioma cells had no inhibitory effect on the growth of primary or immortalized human astrocytes (Figure S3C).

To further investigate the bystander effect, the recipient cells treated with CM from the edited donor cultures were evaluated for cell-cycle progression and cell death. GSCs and glioma cells grown in G1-CM or G3-CM exhibited 2- to 6.5-fold higher accumulation in the sub-G1 phase relative to the cells grown in either EV-CM or CM from untreated cells (UT-CM) (Figures 1H and S3D). Quantification of cell death in these cultures demonstrated that G1-CM and G3-CM exposure leads to a 2- to 8.5-fold increase in the levels of annexin V$^+$/7-AAD$^+$ cells (Figures 1I and S3E). Altogether, these results indicate that factors released by the miR-10b-edited glioma cells and present in G1-CM and G3-CM inhibit the proliferation and induce cell death of naive glioma cells.

Identification of miR-10b-regulated cell death promoting secreted compounds

To investigate the secreted factors mediating the observed effect, we first pre-incubated CM samples from miR-10b-edited GSCs in the presence or absence of RNase before using them for culturing naive recipient cells. Incubation with RNase did not change the growth-inhibitory effect of the CM from miR-10b-edited GSCs (Figure S4), suggesting that the bystander effect of miR-10b editing is not induced by RNA.

To identify the death-promoting compound(s) secreted by miR-10b-edited cells, we sequentially fractionated G1-CM and EV-CM collected from GBM8 cells using Amicon filters with 100-, 50-, 30-, 10-, and 3-kDa pores. The fractions have been added to naive GBM8 cells and their effects on GSC growth monitored. Various CM fractions derived from the edited cells affected GSC growth to a different extent. The fractions of 30–50 and <10 kDa exhibited 7- and 2-fold inhibitory capacity, respectively (Figure 2A). These experiments suggested that major death-promoting compound(s) are proteins smaller than 50 kDa.

To further confirm this conclusion, the G1-CM, G3-CM, and EV-CM samples from additional glioma lines and GSCs (U251, GBM8, and GBM4) were gel filtrated by size to remove proteins larger than

miR-10b-edited (G1, G3) LN229 and U251 or Cas9-only (EV) control cultures. Cell viability was assessed by WST-1 assay (mean ± SD, n = 5 samples/group, one-way ANOVA). (G) Naive GBM8 cells were cultured for 7 days in the CM derived from the corresponding miR-10b-edited GBM8 cultures and the resulting spheroids analyzed. Representative bright-field images and data quantification are demonstrated (mean ± SEM, n = 5 samples/group, One-way ANOVA). (H and I) Glioma cells and GSCs were cultured in CM from the indicated corresponding donor cells, followed by flow cytometry analysis of cell cycle (H) and annexin V and 7-AAD staining (I), and the data quantification is presented (mean ± SEM, n = 3 samples/group, two-tailed unpaired t test). *$p < 0.05$, **$p < 0.01$, ***$p < 0.001$, ****$p < 0.0001$, ns, not significant.

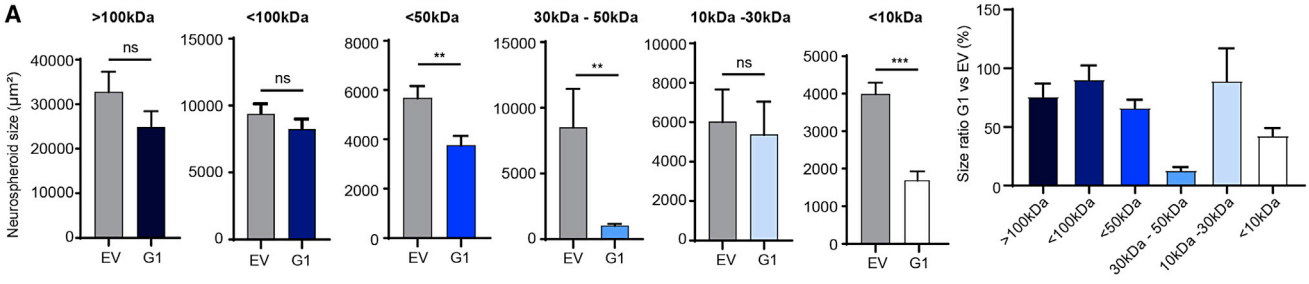

B

Gene Symbol	Description	Protein size	Number of unique peptides	Upregulation score	Maximal upregulation
AGRN	Isoform 3 of Agrin	110, 90, 22 kDa	9	15	8.5
BSG	Isoform 2 of Basigin	42.2 kDa	5	14	3.9
C21orf33	ES1 protein homolog, mitochondrial	28.1 kDa	4	21	10.3
CFL1	Cofilin-1	18.5kDa	3	5	3.8
CXADR	Coxsackievirus and adenovirus receptor	40 kDa	2	6	5.2
IGFBP2	Insulin-like growth factor-binding protein 2	35 kDa	3	7	4.2
IGFBP5	Insulin-like growth factor-binding protein 5	30.5 kDa	4	5	2.4
NOV/IGFBP9	Protein NOV homolog	40kDa	3	6	12.1
NPTX2	Neuronal pentraxin-2	47 kDa	6	11	14.7
PCNA	Proliferating cell nuclear antigen	28kDa	12	25	23.7
PGK1	Phosphoglycerate kinase 1	45kda	17	41	20.8
TXN	Thioredoxin	11.5kDa	8	14	47.2

Figure 2. Identification of cell-death-promoting secreted compounds by mass spectrometry

(A) Sequential fractionation of CM derived from miR-10b-edited GSCs identifies the fractions with growth-inhibitory properties. The CM samples collected from naive or edited GBM8 cells were size fractionated, and the fractions added to the recipient GBM8 cultures. The growth of GSC spheroids was monitored, and the spheroid's size is demonstrated (mean ± SEM, n = 5 samples/group, one-way ANOVA). The right panel depicts the relative effects of the indicated fraction to the corresponding EV control. $^{**}p < 0.01$, $^{***}p < 0.001$, ns, not significant. (B) Top proteins in which secretion is upregulated in CM of miR-10b-edited cells, identified by quantitative TMT mass spectrometry. The protein's size, number of unique peptides per protein detected, and the maximal peptide-level upregulation are indicated. The data were normalized to control samples treated with Cas9 only (EV-CM), n = 4 samples/group. The protein-level "upregulation score" was defined as the total number of peptide hits upregulated >1.75-fold.

50 kDa. The eluted fractions below 50 kDa were combined, and their growth-inhibitory activity was further validated (Figure S5). The corresponding BSA-depleted G1-CM, G3-CM, and EV-CM fractions below 50 kDa were analyzed by quantitative tandem mass tag (TMT) mass spectrometry. The mass spectrometry (MS) spectra of the secretome were analyzed by the SEQUEST algorithm against the Uniprot protein database. We detected 3,124 peptides representing 577 proteins (with 1% false discovery rate [FDR]) commonly secreted by three glioma cell types. Among them, several candidates whose levels were upregulated in both G1-and G3-edited glioma CM, with multiple peptides per protein showing similar patterns, have been identified (Figure 2B).

We further focused on two protein candidates, PGK1 and IGFBP2, based on their established extracellular functions.[18,19] The elevated levels of PGK1 and IGFBP2 in the CM of miR-10b-edited glioma cells have been validated using western blot analysis (Figure 3A). Of note, while a single PGK1 bend was detected in the CM of most glioma cultures, several IGFBP2 variants were detected, all exhibiting similar pattern (Figure 3A). Further analysis of glioma cell lysates demonstrated that PGK1 and IGFBP2 levels were also upregulated in miR-10b-edited cells (Figure S6), indicating that not only their secretion but also their expression are regulated by miR-10b.

In silico analysis of PGK1 and IGFBP2 mRNAs identified both canonical (seed-containing) and non-canonical miR-10b-binding sites in the PGK1 and IGFBP2 3′ UTRs and additional sites in the IGFBP2 ORF and 5′ UTR (Table S1).[20] As miR-10b has an established non-canonical binding activity,[7,21] we considered multiple putative binding sites and tested them for the direct binding and regulation by miR-10b using PGK1 and IGFBP2 fragments subcloned into psiCheck2 luciferase reporter vectors. Two reporters have been constructed for PGK1 and four reporters for IGFBP2 (corresponding to three alternative mRNA variants and their shared sequence). The miR-10b reporter with a perfect complementary site was utilized as a positive control.[5] The analysis was performed on MCF7 cells expressing low endogenous levels of miR-10b in the absence or presence of synthetic miR-10b. It demonstrated that miR-10b triggered a robust reduction in the activities of both PGK1 and IGFBP2 reporters (except the minor 5′ UTR V2 variant of the IGFBP2) (Figures 3B and 3C). Collectively, these data indicate that miR-10b directly regulates the expression of highly secreted PGK1 and IGFBP2 and that miR-10b editing leads to the enhanced secretion of these factors in the extracellular space.

PGK1 and IGFPB2 promote the death of glioma cells

To investigate whether secreted PGK1 and/or IGFBP2 may mediate the observed bystander effect of miR-10b editing, we tested the activity of recombinant PGK1 and IGFBP2 proteins on glioma cells. Titration experiments suggested that after editing, the GSCs secrete about an additional 4 and 5.8 ng/µL PGK1 and IGFBP2, respectively

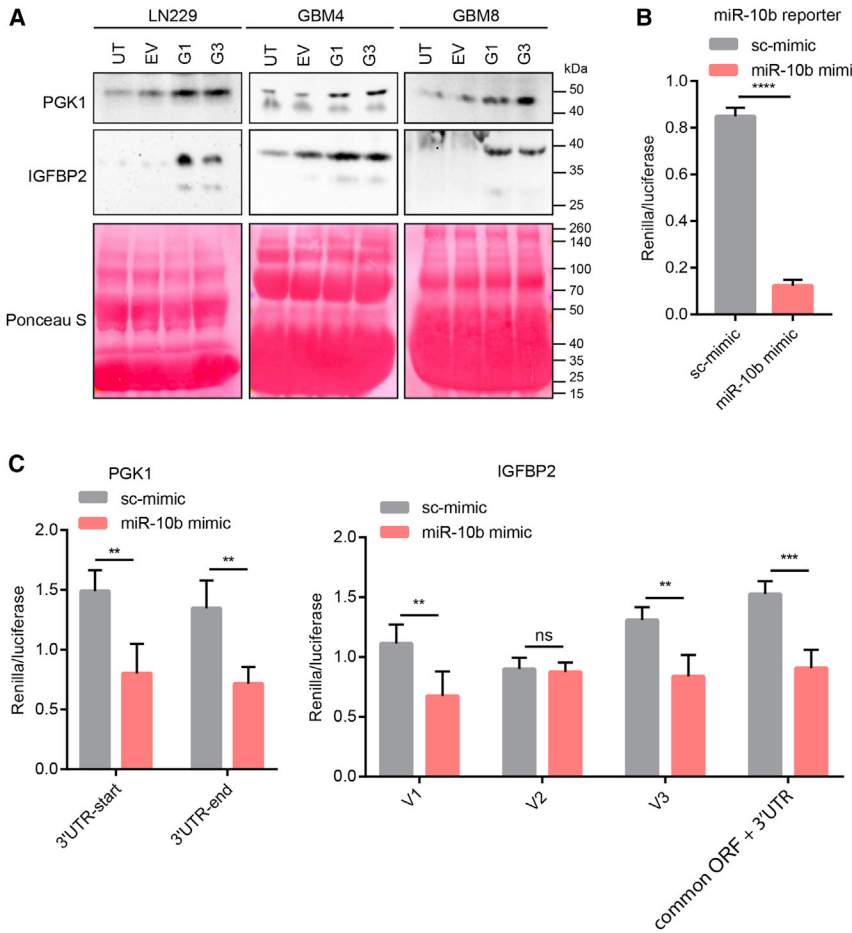

Figure 3. PGK1 and IGFBP2 are secreted miR-10b targets

(A) The levels of PGK1 and IGFBP2 proteins are increased in CM of miR-10b-edited GSCs and glioma cells. Naive GBM8, GBM4, and LN229 cells were transduced with either EV (Cas9 only), G1, or G3 (miR-10b-editing) lentivirus, or UT, for 5 days, and the CM samples collected and analyzed by western blotting. Ponceau S staining was used as loading control. (B) miR-10b mimic regulates luciferase reporter containing a single miR-10b complementary site (mean ± SD, n = 5 samples/group, two-tailed unpaired t test). Scramble mimic (sc-mimic) was used as a control. (C) miR-10b mimic reduces the activity of luciferase reporters of PGK1 and IGFBP2 with several putative miR-10b-binding sites (mean ± SD, n = 5 samples/group, two-tailed unpaired t test). The detailed description of specific reporter constructs is in the materials and methods. **p < 0.01; ***p < 0.001; ****p < 0.0001; ns-not significant.

(Figure S7). Thus, serially diluted human recombinant proteins (at 0–6 ng/μL) were added to the growth media of glioma cells and GSC cultures. The addition of the rhPGK1 to GBM8, GBM4, and LN229 cells resulted in a dose-dependent inhibitory effect on the cell growth. The viability of LN229 was inhibited by 1.5–6 ng/μL PGK1 by 40% (Figure 4A). The ability of GBM8 and GBM4 cells to form full-size spheroids was also strongly reduced (Figure 4B). Furthermore, treatment of glioma cells and GSCs with 6 ng/μL rhPGK1 induced their cell death 5- to 15-fold as indicated by the cell-cycle analysis and accumulation of annexin $V^+/7ADD^+$ (Figures 4C and 4D). The addition of rhIGFBP2 to glioma and GSC cultures led to similar, albeit less pronounced, effects on spheroid formation, cell growth, and cell death.

To further confirm the roles of extracellular IGFBP2 and PGK1 in glioma cell death, we conducted rescue experiments using their specific inhibitors. CM samples derived from miR-10b-edited GSCs and the corresponding control cells were pre-incubated with either IGFBP2 neutralizing antibody or CBR-470-1, a small molecule PGK1 inhibitor, and the effect of these CM on the growth of naive GBM8 spheroids was analyzed. Both the PGK1 inhibitor and IGFBP2 neutralizing antibody reduced the growth inhibitory effect of the G1-CM and G3-CM (Figure 5). Altogether, the data indicate that miR-10b targets PGK1 and IGFBP2, whose secretion is enhanced by miR-10b editing; mediate the observed bystander effect; and promote the non-autonomous cancer cell death in the edited GBM.

DISCUSSION

Multiple therapeutic strategies and clinical trials for GBM turned unsuccessful (reviewed in Alexander and Cloughesy[4] and Krichevsky and Uhlmann[22]). However, the last decade of neuro-oncology genomic, transcriptomic, and epigenetic research expanded the repertoire of molecular targets beyond the conventional RTK and angiogenesis inhibitors and immunotherapies.[4] It also challenged the perception of cancer drivers as exclusively proteinaceous factors. Regulatory RNA, and most notably miRNAs, have been firmly associated with carcinogenesis and are now actively pursued as druggable therapeutic targets for various indications in oncology (reviewed in Mishra et al.[23] and Rupaimoole and Slack[24]).

With the tremendous need for common molecular targets and new therapies for heterogeneous malignant gliomas, miR-10b presents a unique and promising target. It is expressed in almost all malignant gliomas and exhibits characteristics of the major regulator essential for glioma growth and viability. The specificity of miR-10b expression in glioma and its absence in the normal neuroglial cells of the brain lay the foundation for highly potent, selective, and non-toxic targeting.[7,10] While oligonucleotide-based miRNA inhibition remains challenging due to the poor delivery and distribution of antisense oligonucleotides (ASOs) in the brain tumor, miR-10b gene editing may provide an alternative targeting strategy.[10] The major advantage of the gene editing approach is the permanent nature of miR-10b ablation in the tumor and particularly in the GSC

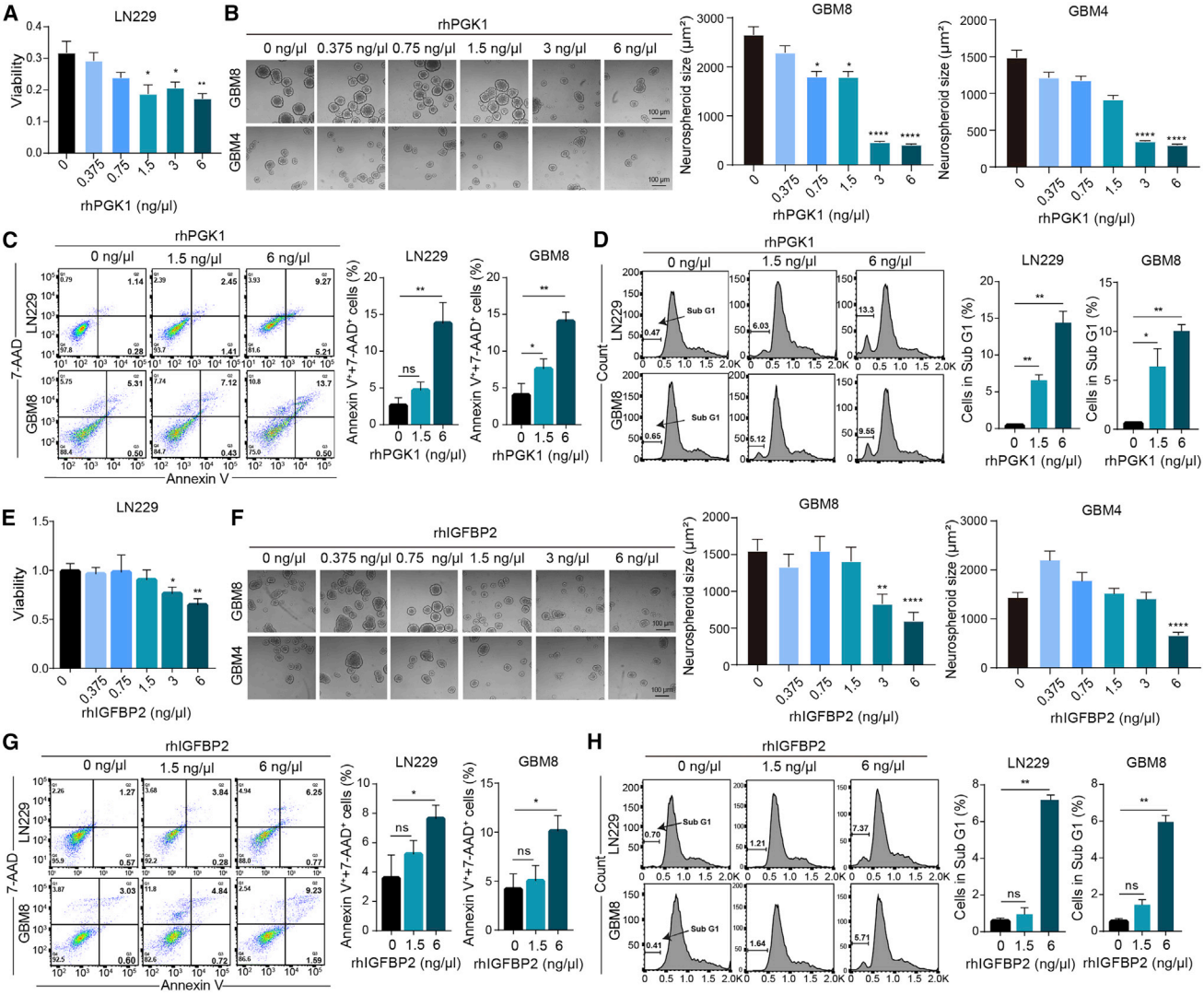

Figure 4. PGK1 and IGFPB2 promote glioma cell death

(A) Recombinant human PGK1 (rhPGK1) inhibits the growth of glioma cells. Sequentially diluted rhPGK1 was added to LN229 cultures, and cell viability was evaluated after 7 days by WST-1 assays (mean ± SEM, n = 5 samples/group, one-way ANOVA). (B) Recombinant hPGK1 inhibits the growth of GSCs. Sequentially diluted rhPGK1 was added to GBM8 and GBM4 cells and their growth monitored over 7 days and the resulting spheroids analyzed. Representative bright-field images and data quantification are demonstrated (mean ± SEM, n = 3 samples/group, one-way ANOVA). (C and D) LN229 and GBM8 cells were treated with recombinant hPGK1 for 5 days, followed by annexin V and 7-AAD staining (C) and cell-cycle (D) quantitative flow cytometry analysis (mean ± SEM, n = 3 samples/group, two-tailed unpaired t test). (E) Recombinant hIGFBP2 inhibits the growth of glioma cells. Sequentially diluted rhIGFBP2 was added to LN229 cultures, and cell viability was evaluated after 7 days by WST-1 assays (mean ± SD, n = 3 samples/group, two-tailed unpaired t test). (F) Recombinant hIGFBP2 inhibits the growth of GSCs. Sequentially diluted rhIGFBP2 was added to GBM8 and GBM4 cells and their growth monitored over 7 days and the resulting spheroids analyzed. Representative bright-field images and data quantification are demonstrated (mean ± SEM, n = 3 samples/group, two-tailed unpaired t test). (G and H) LN229 and GBM8 cells were treated with recombinant hIGFBP2 for 5 days, followed by annexin V and 7-AAD staining (G) and cell-cycle (H) quantitative flow cytometry analysis (mean ± SEM, n = 3 samples/group, two-tailed unpaired t test). *p < 0.05, **p < 0.01, ****p < 0.0001, ns, not significant.

population that is most chemotherapy and radiotherapy resistant. Since glioma cells exhibit miR-10b dependence, its loss is detrimental to the viability of tumor cells but non-toxic for normal neural cells of the brain.[10] Thus, miR-10b gene editing holds a great promise for GBMs. The first *ex vivo* and *in vivo* CRISPR gene editing therapies have just been approved for human pathologies,[25–27] and there are multiple pre-clinical efforts on therapeutic gene editing for various cancers.[28] As a critical unmet need, GBMs may pave the way for *in vivo* gene editing therapy in clinical oncology. However, the GBM-targeting drugs must be highly potent since any therapy-escaping cells may almost inevitably lead to tumor recurrence. Can the CRISPR-Cas9 system be delivered throughout

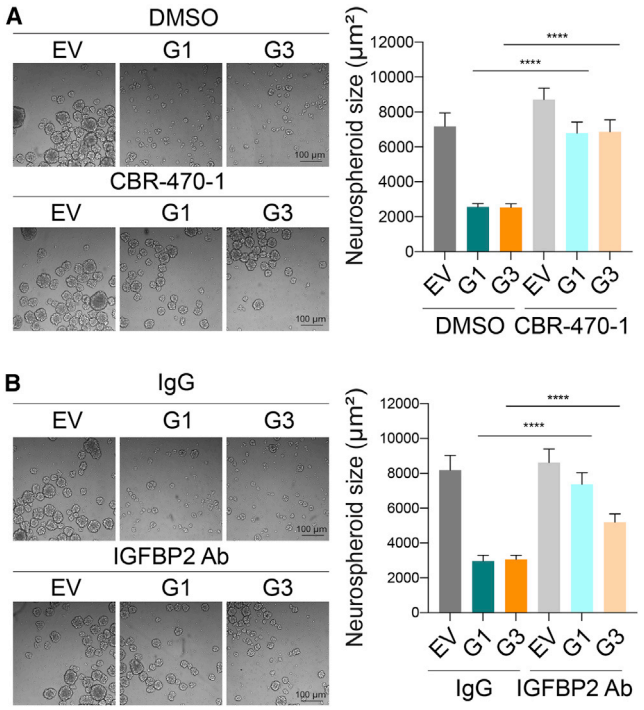

Figure 5. PGK1 and IGFBP2 mediate bystander effects of miR-10b editing

(A) CM samples derived from miR-10b-edited GBM8 cultures (G1 and G3) and the corresponding EV control cells were incubated with PGK1 inhibitor CBR-470-1 (10 μM) or DMSO and used for culturing naive GBM8 for 7 days. Representative microscopy images are shown. The effects on GSC growth were quantified (right panel, mean ± SEM, n = 3 samples/group, two-tailed unpaired t test). (B) CM derived from miR-10b-edited GBM8 cultures (G1 and G3) and the corresponding EV control cells were incubated with 10 μg/mL anti-IGFBP2 neutralizing antibody or control goat IgG and used for culturing naive GBM8 for 7 days (mean ± SEM, n = 3 samples/group, two-tailed unpaired t test). **** $p < 0.0001$.

the tumor and target all tumor cells even if locally infused via neurosurgery at the time of tumor resection? It may not be feasible if nearly 100% targeting efficiency is required.

Here, we report that miR-10b gene editing in glioma cells, induced by two alternative sgRNAs, triggers a potent bystander effect leading to the cell death of naive unedited glioma cells, including the GSCs. This effect was observed in mixed glioma spheroid cultures and induced by the CM derived from the heterogeneous edited glioma cells, implying the involvement of secreted factors. Since the CM was cleared of the lentiviral particles employed as editing vehicles, it was also depleted in extracellular vesicles (which are larger than 100 nm, similar to lentiviruses).[29,30] Moreover, treatment of the CM with RNase has not reduced the bystander effect, suggesting that is it mediated by proteins rather than RNA. Using MS analysis, we identified two new miR-10b targets, PGK1 and IGFBP2, whose expression and secretion from glioma cells were augmented by miR-10b ablation. Both PGK1 or IGFBP2 mRNAs have multiple miR-10b-binding sites, canonical and non-canonical, as was commonly observed for other miR-10b targets.[10,31,32]

PGK1 is a multifunctional "moonlighting" protein, and its role in cellular metabolism and tumorigenesis has been widely studied (reviewed in Pickard and McCance[19] and Rojas-Pirela et al.[33]). In the mitochondria, it converts 1,3-diphosphoglycerate to 3-phosphoglycerate as part of the TCA cycle.[34,35] Thus, it is an essential enzyme in the aerobic glycolysis pathway, and its high intracellular expression promotes tumor cell proliferation. However, the high levels of extracellular PGK1 suppress cancer malignancy, partly due to its ability to bind other proteins[36–38] and reduce disulfide bonds.[39,40] For example, PGK1 behaves as a tumor suppressor by reducing disulfide bonds in plasmin, thereby suppressing angiogenesis.[39,41,42] PGK1 also interacts with and activates Beclin1, thereby promoting autophagy.[43] Non-cell-autonomous functions of PGK1 in glioma, particularly the growth-suppressing mechanism(s) of the secreted PGK1 on glioma cells, remain to be further investigated.

IGFBP2 is also a multifunctional protein that contains IGF-1, IGF-2, integrin-α5, and heparin-binding domains (reviewed in Clemmons[44]). The tumor-suppressive functions of IGFBP2 are mostly associated with its ability to bind IGFs, prevent their receptor binding, and thereby repress the IGF-driven tumorigenesis.[45–47] Oncogenic properties of IGFBP2 that are generally IGF independent were also reported.[48,49] Here, we demonstrate that extracellular IGFBP2, whose secretion from glioma is enhanced by miR-10b editing, reduces the growth of GSCs. However, the mechanisms mediating the effects of both PGK1 and IGFBP2 on GSCs require further investigation. Of note, the incomplete rescue provided by PGK1 and IGFBP2 inhibitors, as well as established functions of miR-10b in controlling diverse signaling pathways in glioma,[5–7,10,21,50] suggest that additional factors released by miR-10b-edited cells may contribute to the observed bystander mechanism. Overall, our findings demonstrate that miR-10b editing reduces the growth of glioma cells in both autonomous and non-autonomous ways, further supporting its potential for GBM therapy development.

MATERIALS AND METHODS

Cell cultures

Human glioma LN229, U251, and breast cancer MCF7 cell lines cells were obtained from ATCC (2005–2007) and maintained in DMEM (Gibco) supplemented with 10% fetal bovine serum (FBS; Gibco) and 1% penicillin/streptomycin solution.[5] Adherent cells were passaged by trypsinization with 0.25% trypsin/EDTA (Gibco). Human low-passage GSCs GBM8 and GBM4 were a generous gift from Dr. Hiroaki Wakamoto, MGH. The GSCs were cultured as neurospheres in serum-free neurobasal medium (Gibco) supplemented with 3 mM GlutaMAX (Gibco); 1× B-27 (Invitrogen); 0.5× N-2 (Invitrogen); 20 ng/mL EGF (R&D Systems, Minneapolis, MN, USA); and 20 ng/mL FGF (PeproTech, Cranbury, NJ, USA), as previously described.[51] The cells were passaged by dissociation using NeuroCult Chemical Dissociation Kit-Mouse (StemCell Technologies, Vancouver, BC, Canada) following the manual. Primary human astrocytes from fetal female cortical tissues were provided by Advanced Bioscience Resources (Alameda, CA, USA) and cultured in DMEM/F-12 supplemented with

10% FBS and 1% penicillin/streptomycin solution, as previously described.[52] For immortalized cultures, primary human astrocytes were transduced after two passages by the cocktail of SV40 large T antigen (SV40), RasG12V (Ras), and TERT lentiviruses for 3 consecutive days. Human cells were used in accordance with the policies of institutional review boards at Brigham and Women's Hospital.

Production of CRISPR-Cas9 lentiviruses

CRISPR-Cas9 miR-10b editing lentiviral vectors have been produced as previously described.[10] Briefly, the G1 and G3 sgRNA guide sequences were cloned into lentiCRISPR v.2 plasmid (a gift from Feng Zhang, Addgene plasmid #52961) based on Sanjana et al.[53] and Cong et al.[54] For lentivirus production, the lentiCRISPR v.2 plasmids were co-transfected with packaging psPAX2 plasmids and pMD2.G envelope-expressing plasmid (Addgene plasmids #12259 and #12260) as described,[53] and viruses were concentrated by additional ultracentrifugation at 25,000 RPM. Functional viral titers were determined by serial dilution in glioma cells using immunofluorescence for Cas9 with anti-Cas9 antibody (7A9-3A3, Novus Bio, Littleton, CO, USA) 1:300. Positive cells were counted, and the titers were estimated using the following formula: titer (TU/mL) = (number of cells transduced × percent fluorescent × dilution factor)/(transduction volume in mL).

CM preparation, cell infection, and treatment

For CM preparation, glioma cells were seeded at 2×10^6 cells/well in 6-well plates. The adherent LN229 and U251 cells were transduced with lentivirus (4×10^5 TU/mL) 24 h after plating, while GSC spheroids were dissociated to single cells before infection. The cells were incubated with either CRISPR-Cas9 (EV) or CRISPR-Cas9 gRNAs (G1 or G3) lentiviruses for 4–5 days. The CM was then collected, centrifuged for 15 min at 2,000 × *g* to remove cells and cell debris, and further filtered through a 0.1-μm filter to remove any traces of the virus. The adherent recipient cultures were seeded at 3.5×10^3 cells/well in 96-well plates 24 h prior to addition of the CM. Naive GSC spheres were dissociated to single cells, resuspended in the corresponding CM, and seeded in 96-well plates at 3.5×10^3 cells/well. The cells were incubated in the CM for 7–9 days in standard culture conditions. For experiments with the recombinant proteins, sequential dilutions of human recombinant proteins PGK1 (5455-PK-010, R&D Systems) and IGFBP2 (674-B2-025, R&D Systems) were prepared in the mixed fresh media and CM derived from naive glioma cells cultured for 5 days at a 3:7 ratio.

For the rescue experiments, CM samples derived from the miR-10b-edited GSCs and the corresponding control cultures were incubated with 10 μg/mL IGFBP2-neutralizing antibody (R&D Systems, AF674)[55] or control goat immunoglobulin G (IgG; Sigma) at 37°C for 4 h. The antibody has been removed from CM by using Dynabeads Protein G (Invitrogen, 10003D) via overnight rotation, and the CMs were used for culturing naive GSCs over 7 days. For PGK1 inhibition, CM samples were incubated with 10 μM PGK1 inhibitor CBR-470-1 (R&D Systems)[56,57] or DMSO at 37°C for 8 h. For RNase treatment, CMs derived from the miR-10b-edited GSC cultures were treated with RNase A (Affymetrix/USB 70194Y; 1:500 dilution) at 37°C for 5 min, and CMs were then used for culturing the recipient GCSs.

Mixed cultures

GSCs were dissociated and plated in 24-well plates at 1×10^5 cells/well concentration. The cells were infected with lentivirus (4×10^5 TU/mL) and incubated with either lentiviral CRISPR-Cas9 (EV) or lentiviral CRISPR-Cas9 gRNAs (G1 or G3) for 24 h. The cells were then pelleted, washed with 1× DPBS, mixed with UT GBM8 mCherry$^+$ cells at a 1:1 ratio, plated in fresh growth media, and cultured for 7 days.

Western blot analysis

Cells were pelleted, washed in DPBS (Gibco), and lysed with ×2 radioimmunoprecipitation (RIPA) buffer (Boston BioProducts, Milford, MA, USA) supplemented with protease inhibitor cocktail (Roche Diagnostics). CM samples were concentrated using 3K Amicon Ultra Centrifugal Filters (Millipore Sigma). Protein concentrations of cell lysates and concentrated CM were measured using a Micro BCA protein assay kit (Pierce Biotechnology), and 50-μg protein per lane was resolved on SDS-PAGE (Invitrogen), followed by the immunoblot detection and visualization with enhanced chemiluminescent (ECL) western blotting detection reagents (Pierce Biotechnology). Immunoblotting was performed with the following primary antibodies: anti-IGFBP2 (Abcam, ab188200, 1:1,000 dilution), anti-PGK1 (LSBio, LS-C373462, 1:500 dilution), and anti-tubulin (Abcam, ab6160, 1:5,000 dilution).

Fractionation of CM

CM from GBM8 cells, transduced with either CRISPR-Cas9 (EV) or CRISPR-Cas9 gRNAs (G1) lentiviruses (4×10^5 TU/mL), have been collected 5 days post-infection and cleared from cell debris and virus by centrifugation (2,000 × *g*, 15 min) and filtration using 0.1-μm filters. The CM samples were then fractionated with 100, 50, 30, and 10 K cut-off Amicon Ultra Centrifugal Filters (Millipore Sigma) to produce >100, <100, 50–100, <50, 30–50, <30, and 10–30 kDa concentrates. The samples collected from the flow-through and on-filter concentrates were reconstituted to their initial volume with neurobasal medium (Gibco). 100 μL of each fraction was added in triplicate to naive GBM8 cells seeded in 96-well plates.

Sample preparation and MS

For MS, the CM samples were prepared as following: CM from glioma cells transduced with either CRISPR-Cas9 (EV) or CRISPR-Cas9 gRNAs (G1 or G3) lentiviruses (4×10^5 TU/mL) were collected 5 days post-infection and cleared from cell debris and virus. Each CM sample was concentrated to 500 μL, loaded on Superdex 75 Increase 10/300 GL column (GE, 29148721) using a 500-μL loop, and eluted with 20 mM TRIS, 150 mM NaCl pH 6.5 (at room temperature [RT])/7.3 (at 4°C) at a flow rate of 0.25 mL/min at 4°C. 300-mL elution fractions were collected. Gel filtration standard (151–1901, Bio-Rad) was utilized in parallel. The fractions corresponding to proteins smaller than 50 kDa were merged, concentrated with 3 K cut-off Amicon Ultra Centrifugal Filter (Millipore Sigma) to

500-mL samples, and subjected to additional albumin depletion using Aurum Affi-Gell Blue columns (BioRad) following the manufacturers' instructions.

The samples have been then prepared, labeled, and subjected to the quantitative TMT MS analysis at the Thermo Fisher Scientific Center for Multiplexed Proteomics at Harvard Medical School, as previously described.[58,59] Briefly, an equal volume (500 mL) of 8 M urea lysis buffer in 200 mM EPPS (pH 8) with protease and phosphatase inhibitors was added to each sample, reduced with 5 mM TCEP for 20 min at RT, and alkylated with 15 mM iodoacetamide for 20 min in the dark. The samples were TCA precipitated, and the pellets were resuspended in 200 mM EPPS (pH 8) and digested at RT for 14 h with Lys-C protease (FUJIFILM Wako) at a 50:1 protein-to-protease ratio. Trypsin was then added at a 100:1 protein-to-protease ratio, and the reactions were incubated for 6 h at 37°C.

The samples were labeled with TMTpro reagents (Thermo Fisher Scientific) according to the manufacturer instructions. Labeling reactions were quenched with 0.5% hydroxylamine for 15 min followed by acidification with TFA. Reactions were combined, cleaned by SepPak, and dried by speedvac. The sample was fractionated into 6 fractions using Pierce High pH Reversed-Phase Peptide Fractionation Kit (Thermo Fisher Scientific). resuspended in 5% ACN/5% FA, and analyzed on Orbitrap Fusion Lumos Tribird mass spectrometer (Thermo Fisher Scientific) equipped with a Thermo Easy-nLC 1200 for online sample handling and peptide separations using an LC-MS2 method. MS spectra were searched using the SEQUEST algorithm against a Uniprot composite database. Peptide spectral matches were filtered to a 1% FDR using the target-decoy strategy combined with linear discriminant analysis. The proteins were filtered to a <1% FDR. Proteins were quantified only from peptides with a summed signal-to-noise (SN) threshold of $\geq$100 and MS2 isolation specificity of 0.5.

The total signal for each TMT channel was calculated, and the raw data were normalized as follows. Normalization factors were calculated so that the total signal in each TMT channel was equal to the lowest channel. The raw signal to noise for each peptide was divided by the normalization factor for each TMT channel. The normalized data for each peptide, for G1- and G3-edited samples, was further divided by the normalized data for control EV samples.

Proliferation and cell growth assays

Cell viability of adherent cells was measured by WST-1 proliferation assay (Roche, 11644807001) or CellTiter- Glo Luminescent cell viability assay (Promega, Madison, WI, USA) for GSCs, using GloMax Explorer instrument (Promega, G9242), according to the manufacturer's instructions. GSC spheroids were analyzed by scanning the wells in InCell Analyzer 2200 (GE), stitching the pictures to obtain full-well images, and measuring the spheroids' size using Fiji Image J software (NIH, open source). Generally, the experiments were repeated at least three times for each experimental condition.

Flow cytometry analysis

For the cell-cycle analysis, cells were collected, washed 3 times with 1× DPBS, fixed, and permeabilized with 75% ethanol at −20°C overnight. The cells were further incubated with 5 μM PI (Sigma) or Vybrant DyeCycle Violet stain (Thermo Fisher Scientific, V35003) for 30 min at 37°C, followed by the flow cytometry analysis using the BD LSRII analyzer. The percentage of sub-G1 was monitored using FlowJo software (v.10.8.1). Annexin V and 7-AAD staining (BD Biosciences, 559763) was performed according to the manufacturer's instructions. Briefly, the cells were collected by centrifugation, resuspended in 500 μL 1× annexin V binding buffer, incubated with 5 μL annexin V and 5 μL 7-AAD at RT for 15 min in the dark, and followed by the flow cytometry analysis.

Immunofluorescence

The cells were washed with 1× DPBS and collected by centrifugation. They were then fixed with 4% paraformaldehyde (PFA), permeabilized with 0.1% Triton X-100 in PBS, and blocked in 5% BSA for 1 h. The cells were incubated with primary antibodies (mouse anti-CRISPR Cas9, Novus Biologicals, NBP2-36440, 1:200 dilution) overnight at 4°C and further incubated with the secondary antibody (goat anti-mouse Alexa Fluor 488, Invitrogen, 1:200 dilution). The nuclei were stained with DAPI (1:1,000). The staining was visualized and imaged using Zeiss LSM710 confocal microscopy.

Luciferase reporter assay

PsiCHECK2 miR-10b reporter with a perfect miR-10b-binding site has been produced as previously reported.[7] The IGFBP2 (NM_000597.3) open reading frame (ORF) was cloned into psiCHECK2 (Promega) downstream of *Renilla* luciferase using the SgfI and PmeI restriction enzymes sites from pCMV6-XL4-IGBMP2 (#SC119778, Origine). Other fragments of IGFBP2 mRNA (including the ORF and the UTRs) and the PGK1 3′ UTR have been amplified with primers listed in Table S2 and cloned using the TOTO PCR kit (Invotrogen), cut with SgfI and PmeI restriction enzymes, and cloned into psiCHECK2 (Promega) downstream of *Renilla* luciferase. The following fragments containing miR-10b putative binding sites have been produced: PGK1 (NM_000291.4) 2,421–3,190 (3′ UTR start) and 4,115–4,430 nt (3′ UTR end); IGFBP2 (NM_000597.3) 181–206 (V1) and 916–1,396 nt (common ORF + 3′ UTR); IGFBP2 (NM_001313990.2) 1–180 nt (V2); and IGFBP2 (NM_001313992.2) 1–423 nt (V3).

For the reporter assays, MCF7 cells were seeded at 5,000 cells/well in 96-well plates and co-transfected with 100 ng psiCHECK-2 luciferase reporters and either 50 nM miR-10b mimic or scramble mimic control (Ambion, Dharmacon). Luciferase luminescence was measured 24 h after transfection using Dual-Glo Luciferase Assay (Promega E2920) and GloMax explorer instrument (Promega). *Renilla* luciferase activity was normalized to the *Firefly* luciferase activity.

Statistical analysis

Values are given as mean ± SEM or as mean ± SD. Numbers of experimental replicates are given in the figure legends. When two groups were compared, significance was determined using an unpaired,

non-parametric two-sided t test, and normal distribution was verified by one-sample Kolmogorov-Smirnov test. For more than two-group comparison, significance was determined using one-way ANOVA non-parametric test (Kruskal-Wallis).

DATA AVAILABILITY

All data needed to evaluate the conclusions in the paper are present in the paper and/or the supplemental information. Additional data related to this paper may be requested from the authors.

SUPPLEMENTAL INFORMATION

Supplemental information can be found online at https://doi.org/10.1016/j.omtn.2022.12.018.

ACKNOWLEDGMENTS

We thank the NeuroTechnology Studio and Dr. Lai Ding at Brigham and Women's Hospital for providing instrument access and consultation on data acquisition and analysis. We also thank the Thermo Fisher Scientific Center for Multiplexed Proteomics at Harvard Medical School, and specifically Drs. Mark Jedrychowski and Rachel Rodrigues, for MS data generation and consultation. This work was supported by NIH R01 CA215072 and R01 NS113929 grants to A.M.K. L.P. was supported by AG073341 award from NIA.

AUTHOR CONTRIBUTIONS

A.M.K. and R.R. conceived and designed the study; R.R. and Y.Z. performed experiments, data analysis, and visualization; L.P. contributed to MS data analysis; Z.W., R.E.F., E.D., B.L., and E.J.U. assisted with experiments and contributed to data analysis; and R.R., Y.Z., and A.M.K. wrote the manuscript. All authors revised and approved the manuscript. A.M.K. acquired funding and supervised the study.

DECLARATION OF INTERESTS

The authors declare no competing interests.

REFERENCES

1. Ostrom, Q.T., Cioffi, G., Waite, K., Kruchko, C., and Barnholtz-Sloan, J.S. (2021). CBTRUS statistical report: primary brain and other central nervous system tumors diagnosed in the United States in 2014-2018. Neuro Oncol. *23*, iii1–iii105.
2. Yan, H., Parsons, D.W., Jin, G., McLendon, R., Rasheed, B.A., Yuan, W., Kos, I., Batinic-Haberle, I., Jones, S., Riggins, G.J., et al. (2009). IDH1 and IDH2 mutations in gliomas. N. Engl. J. Med. *360*, 765–773.
3. Hu, C., Leche, C.A., Kiyatkin, A., Yu, Z., Stayrook, S.E., Ferguson, K.M., and Lemmon, M.A. (2022). Glioblastoma mutations alter EGFR dimer structure to prevent ligand bias. Nature *602*, 518–522.
4. Alexander, B.M., and Cloughesy, T.F. (2017). Adult glioblastoma. J. Clin. Oncol. *35*, 2402–2409.
5. Gabriely, G., Yi, M., Narayan, R.S., Niers, J.M., Wurdinger, T., Imitola, J., Ligon, K.L., Kesari, S., Esau, C., Stephens, R.M., et al. (2011). Human glioma growth is controlled by microRNA-10b. Cancer Res. *71*, 3563–3572.
6. Guessous, F., Alvarado-Velez, M., Marcinkiewicz, L., Zhang, Y., Kim, J., Heister, S., Kefas, B., Godlewski, J., Schiff, D., Purow, B., and Abounader, R. (2013). Oncogenic effects of miR-10b in glioblastoma stem cells. J. Neuro Oncol. *112*, 153–163.
7. Teplyuk, N.M., Uhlmann, E.J., Gabriely, G., Volfovsky, N., Wang, Y., Teng, J., Karmali, P., Marcusson, E., Peter, M., Mohan, A., et al. (2016). Therapeutic potential of targeting microRNA-10b in established intracranial glioblastoma: first steps toward the clinic. EMBO Mol. Med. *8*, 268–287.
8. Lin, J., Teo, S., Lam, D.H., Jeyaseelan, K., and Wang, S. (2012). MicroRNA-10b pleiotropically regulates invasion, angiogenicity and apoptosis of tumor cells resembling mesenchymal subtype of glioblastoma multiforme. Cell Death Dis. *3*, e398.
9. Sun, B., Zhao, X., Ming, J., Liu, X., Liu, D., and Jiang, C. (2019). Stepwise detection and evaluation reveal miR-10b and miR-222 as a remarkable prognostic pair for glioblastoma. Oncogene *38*, 6142–6157.
10. El Fatimy, R., Subramanian, S., Uhlmann, E.J., and Krichevsky, A.M. (2017). Genome editing reveals glioblastoma addiction to MicroRNA-10b. Mol. Ther. *25*, 368–378.
11. Deforzh, E., Uhlmann, E.J., Das, E., Galitsyna, A., Arora, R., Saravanan, H., Rabinovsky, R., Wirawan, A.D., Teplyuk, N.M., El Fatimy, R., et al. (2022). Promoter and enhancer RNAs regulate chromatin reorganization and activation of miR-10b/HOXD locus, and neoplastic transformation in glioma. Mol. Cell *82*, 1894–1908.e5.
12. Filipowicz, W., Bhattacharyya, S.N., and Sonenberg, N. (2008). Mechanisms of post-transcriptional regulation by microRNAs: are the answers in sight? Nat. Rev. Genet. *9*, 102–114.
13. Nicoloso, M.S., Spizzo, R., Shimizu, M., Rossi, S., and Calin, G.A. (2009). MicroRNAs–the micro steering wheel of tumour metastases. Nat. Rev. Cancer *9*, 293–302.
14. Calin, G.A., and Croce, C.M. (2006). MicroRNA signatures in human cancers. Nat. Rev. Cancer *6*, 857–866.
15. Lund, A.H. (2010). miR-10 in development and cancer. Cell Death Differ. *17*, 209–214.
16. Ma, L., Teruya-Feldstein, J., and Weinberg, R.A. (2007). Tumour invasion and metastasis initiated by microRNA-10b in breast cancer. Nature *449*, 682–688.
17. Sheedy, P., and Medarova, Z. (2018). The fundamental role of miR-10b in metastatic cancer. Am. J. Cancer Res. *8*, 1674–1688.
18. He, Y., Luo, Y., Zhang, D., Wang, X., Zhang, P., Li, H., Ejaz, S., and Liang, S. (2019). PGK1-mediated cancer progression and drug resistance. Am. J. Cancer Res. *9*, 2280–2302.
19. Pickard, A., and McCance, D.J. (2015). IGF-binding protein 2 - oncogene or tumor suppressor? Front. Endocrinol. *6*, 25.
20. Rehmsmeier, M., Steffen, P., Hochsmann, M., and Giegerich, R. (2004). Fast and effective prediction of microRNA/target duplexes. RNA *10*, 1507–1517.
21. El Fatimy, R., Zhang, Y., Deforzh, E., Ramadas, M., Saravanan, H., Wei, Z., Rabinovsky, R., Teplyuk, N.M., Uhlmann, E.J., and Krichevsky, A.M. (2022). A nuclear function for an oncogenic microRNA as a modulator of snRNA and splicing. Mol. Cancer *21*, 17.
22. Krichevsky, A.M., and Uhlmann, E.J. (2019). Oligonucleotide therapeutics as a new class of drugs for malignant brain tumors: targeting mRNAs, regulatory RNAs, mutations, combinations, and beyond. Neurotherapeutics *16*, 319–347.
23. Mishra, S., Yadav, T., and Rani, V. (2016). Exploring miRNA based approaches in cancer diagnostics and therapeutics. Crit. Rev. Oncol. Hematol. *98*, 12–23.
24. Rupaimoole, R., and Slack, F.J. (2017). MicroRNA therapeutics: towards a new era for the management of cancer and other diseases. Nat. Rev. Drug Discov. *16*, 203–222.
25. Maeder, M.L., Stefanidakis, M., Wilson, C.J., Baral, R., Barrera, L.A., Bounoutas, G.S., Bumcrot, D., Chao, H., Ciulla, D.M., DaSilva, J.A., et al. (2019). Development of a gene-editing approach to restore vision loss in Leber congenital amaurosis type 10. Nat. Med. *25*, 229–233.
26. Frangoul, H., Altshuler, D., Cappellini, M.D., Chen, Y.S., Domm, J., Eustace, B.K., Foell, J., de la Fuente, J., Grupp, S., Handgretinger, R., et al. (2021). CRISPR-Cas9 gene editing for sickle cell disease and beta-thalassemia. N. Engl. J. Med. *384*, 252–260.
27. Gillmore, J.D., Gane, E., Taubel, J., Kao, J., Fontana, M., Maitland, M.L., Seitzer, J., O'Connell, D., Walsh, K.R., Wood, K., et al. (2021). CRISPR-Cas9 in vivo gene editing for transthyretin amyloidosis. N. Engl. J. Med. *385*, 493–502.
28. Lu, Y., Xue, J., Deng, T., Zhou, X., Yu, K., Deng, L., Huang, M., Yi, X., Liang, M., Wang, Y., et al. (2020). Safety and feasibility of CRISPR-edited T cells in patients

with refractory non-small-cell lung cancer. Nat. Med. *26*, 732–740. https://doi.org/10.1038/s41591-020-0840-5.

29. McCarthy, J.E., Schauder, B., and Ziemke, P. (1988). Post-transcriptional control in Escherichia coli: translation and degradation of the atp operon mRNA. Gene *72*, 131–139.

30. Ma, C., Qi, X., Wei, Y.F., Li, Z., Zhang, H.L., Li, H., Yu, F.L., Pu, Y.N., Huang, Y.C., and Ren, Y.X. (2022). Amelioration of ligamentum flavum hypertrophy using umbilical cord mesenchymal stromal cell-derived extracellular vesicles. Bioact. Mater. *19*, 139–154.

31. Fang, Z., and Rajewsky, N. (2011). The impact of miRNA target sites in coding sequences and in 3'UTRs. PLoS One *6*, e18067.

32. Agarwal, V., Bell, G.W., Nam, J.W., and Bartel, D.P. (2015). Predicting effective microRNA target sites in mammalian mRNAs. Elife *4*, e05005.

33. Rojas-Pirela, M., Andrade-Alviárez, D., Rojas, V., Kemmerling, U., Cáceres, A.J., Michels, P.A., Concepción, J.L., and Quiñones, W. (2020). Phosphoglycerate kinase: structural aspects and functions, with special emphasis on the enzyme from Kinetoplastea. Open Biol. *10*, 200302.

34. Palmai, Z., Seifert, C., Gräter, F., and Balog, E. (2014). An allosteric signaling pathway of human 3-phosphoglycerate kinase from force distribution analysis. PLoS Comput. Biol. *10*, e1003444.

35. Nie, H., Ju, H., Fan, J., Shi, X., Cheng, Y., Cang, X., Zheng, Z., Duan, X., and Yi, W. (2020). O-GlcNAcylation of PGK1 coordinates glycolysis and TCA cycle to promote tumor growth. Nat. Commun. *11*, 36.

36. Boone, T.J., Burnham, C.A.D., and Tyrrell, G.J. (2011). Binding of group B streptococcal phosphoglycerate kinase to plasminogen and actin. Microb. Pathog. *51*, 255–261.

37. Labroussaa, F., Arricau-Bouvery, N., Dubrana, M.P., and Saillard, C. (2010). Entry of Spiroplasma citri into Circulifer haematoceps cells involves interaction between spiroplasma phosphoglycerate kinase and leafhopper actin. Appl. Environ. Microbiol. *76*, 1879–1886.

38. Hu, H., Zhu, W., Qin, J., Chen, M., Gong, L., Li, L., Liu, X., Tao, Y., Yin, H., Zhou, H., et al. (2017). Acetylation of PGK1 promotes liver cancer cell proliferation and tumorigenesis. Hepatology *65*, 515–528.

39. Lay, A.J., Jiang, X.M., Kisker, O., Flynn, E., Underwood, A., Condron, R., and Hogg, P.J. (2000). Phosphoglycerate kinase acts in tumour angiogenesis as a disulphide reductase. Nature *408*, 869–873.

40. Hogg, P.J. (2002). Biological regulation through protein disulfide bond cleavage. Redox Rep. *7*, 71–77.

41. O'Reilly, M.S., Holmgren, L., Shing, Y., Chen, C., Rosenthal, R.A., Moses, M., Lane, W.S., Cao, Y., Sage, E.H., and Folkman, J. (1994). Angiostatin: a novel angiogenesis inhibitor that mediates the suppression of metastases by a Lewis lung carcinoma. Cell *79*, 315–328.

42. Zhou, Z., Yao, H., and Hu, H. (2017). Disrupting tumor angiogenesis and "the hunger games" for breast cancer. Adv. Exp. Med. Biol. *1026*, 171–195.

43. Qian, X., Li, X., Cai, Q., Zhang, C., Yu, Q., Jiang, Y., Lee, J.H., Hawke, D., Wang, Y., Xia, Y., et al. (2017). Phosphoglycerate kinase 1 phosphorylates Beclin1 to induce autophagy. Mol. Cell *65*, 917–931.e6.

44. Clemmons, D.R. (2018). Role of IGF-binding proteins in regulating IGF responses to changes in metabolism. J. Mol. Endocrinol. *61*, T139–T169.

45. Kang, Z., Yu, Y., Zhu, Y.J., Davis, S., Walker, R., Meltzer, P.S., Helman, L.J., and Cao, L. (2014). Downregulation of IGFBP2 is associated with resistance to IGF1R therapy in rhabdomyosarcoma. Oncogene *33*, 5697–5705.

46. Tang, Z., Gillatt, D., Rowe, E., Koupparis, A., Holly, J.M.P., and Perks, C.M. (2019). IGFBP-2 acts as a tumour suppressor and plays a role in determining chemosensitivity in bladder cancer cells. Oncotarget *10*, 7043–7057.

47. Soh, C.L., McNeil, K., Owczarek, C.M., Hardy, M.P., Fabri, L.J., Pearse, M., Delaine, C.A., and Forbes, B.E. (2014). Exogenous administration of protease-resistant, non-matrix-binding IGFBP-2 inhibits tumour growth in a murine model of breast cancer. Br. J. Cancer *110*, 2855–2864.

48. Tombolan, L., Orso, F., Guzzardo, V., Casara, S., Zin, A., Bonora, M., Romualdi, C., Giorgi, C., Bisogno, G., Alaggio, R., et al. (2011). High IGFBP2 expression correlates with tumor severity in pediatric rhabdomyosarcoma. Am. J. Pathol. *179*, 2611–2624.

49. De Marco, C., Laudanna, C., Rinaldo, N., Oliveira, D.M., Ravo, M., Weisz, A., Ceccarelli, M., Caira, E., Rizzuto, A., Zoppoli, P., et al. (2017). Specific gene expression signatures induced by the multiple oncogenic alterations that occur within the PTEN/PI3K/AKT pathway in lung cancer. PLoS One *12*, e0178865.

50. Gabriely, G., Teplyuk, N.M., and Krichevsky, A.M. (2011). Context effect: microRNA-10b in cancer cell proliferation, spread and death. Autophagy *7*, 1384–1386.

51. Wakimoto, H., Mohapatra, G., Kanai, R., Curry, W.T., Jr., Yip, S., Nitta, M., Patel, A.P., Barnard, Z.R., Stemmer-Rachamimov, A.O., Louis, D.N., et al. (2012). Maintenance of primary tumor phenotype and genotype in glioblastoma stem cells. Neuro Oncol. *14*, 132–144.

52. Zeng, A., Wei, Z., Rabinovsky, R., Jun, H.J., El Fatimy, R., Deforzh, E., Arora, R., Yao, Y., Yao, S., Yan, W., et al. (2020). Glioblastoma-derived extracellular vesicles facilitate transformation of astrocytes via reprogramming oncogenic metabolism. iScience *23*, 101420.

53. Sanjana, N.E., Shalem, O., and Zhang, F. (2014). Improved vectors and genome-wide libraries for CRISPR screening. Nat. Methods *11*, 783–784.

54. Cong, L., Ran, F.A., Cox, D., Lin, S., Barretto, R., Habib, N., Hsu, P.D., Wu, X., Jiang, W., Marraffini, L.A., and Zhang, F. (2013). Multiplex genome engineering using CRISPR/Cas systems. Science *339*, 819–823.

55. Phillips, L.M., Zhou, X., Cogdell, D.E., Chua, C.Y., Huisinga, A., R Hess, K., Fuller, G.N., and Zhang, W. (2016). Glioma progression is mediated by an addiction to aberrant IGFBP2 expression and can be blocked using anti-IGFBP2 strategies. J. Pathol. *239*, 355–364.

56. Zheng, J., Zhu, J.L., Zhang, Y., Zhang, H., Yang, Y., Tang, D.R., and Sun, J. (2020). PGK1 inhibitor CBR-470-1 protects neuronal cells from MPP+. Aging *12*, 13388–13399.

57. Bollong, M.J., Lee, G., Coukos, J.S., Yun, H., Zambaldo, C., Chang, J.W., Chin, E.N., Ahmad, I., Chatterjee, A.K., Lairson, L.L., et al. (2018). A metabolite-derived protein modification integrates glycolysis with KEAP1-NRF2 signalling. Nature *562*, 600–604.

58. Li, J., Cai, Z., Bomgarden, R.D., Pike, I., Kuhn, K., Rogers, J.C., Roberts, T.M., Gygi, S.P., and Paulo, J.A. (2021). TMTpro-18plex: the expanded and complete set of TMTpro reagents for sample multiplexing. J. Proteome Res. *20*, 2964–2972.

59. Navarrete-Perea, J., Yu, Q., Gygi, S.P., and Paulo, J.A. (2018). Streamlined Tandem mass tag (SL-TMT) protocol: an efficient strategy for quantitative (Phospho)proteome profiling using Tandem mass tag-synchronous precursor selection-MS3. J. Proteome Res. *17*, 2226–2236.